The EMBO Journal Vol.18 No.4 pp.992–1002, 1999

Loss-of-function mutations in the rice homeobox gene *OSH15* affect the architecture of internodes resulting in dwarf plants

Yutaka Sato, Naoki Sentoku, Yoshio Miura, Hirohiko Hirochika[1], Hidemi Kitano[2] and Makoto Matsuoka[3]

Nagoya University, BioScience Center, Chikusa, Nagoya 464-8601, [1]National Institute of Agrobiological Resources, Tsukuba, 305 and [2]School of Agricultural Science, Nagoya University, Chikusa, Nagoya 464-8601, Japan

[3]Corresponding author
e-mail: j45751a@nucc.cc.nagoya-u.ac.jp

The rice homeobox gene *OSH15* (*Oryza sativa* homeobox) is a member of the *knotted1*-type homeobox gene family. We report here on the identification and characterization of a loss-of-function mutation in *OSH15* from a library of retrotransposon-tagged lines of rice. Based on the phenotype and map position, we have identified three independent deletion alleles of the locus among conventional morphological mutants. All of these recessive mutations, which are considered to be null alleles, exhibit defects in internode elongation. Introduction of a 14 kbp genomic DNA fragment that includes all exons, introns and 5′- and 3′- flanking sequences of *OSH15* complemented the defects in internode elongation, confirming that they were caused by the loss-of-function of *OSH15*. Internodes of the mutants had abnormal-shaped epidermal and hypodermal cells and showed an unusual arrangement of small vascular bundles. These mutations demonstrate a role for *OSH15* in the development of rice internodes. This is the first evidence that the *knotted1*-type homeobox genes have roles other than shoot apical meristem formation and/or maintenance in plant development.
Keywords: dwarf/homeobox/*OSH15*/rice/sclerenchyma

Introduction

The entire above-ground portion of a plant body is an assembly of repetitive units termed phytomers, which consist of an axillary bud, a stem and a leaf. The shoot apical meristem (SAM) continuously produces these units, at the same time maintaining itself as a collection of indeterminate stem cells (Steeves and Sussex, 1989). Recent studies on SAM formation and maintenance in *Arabidopsis* suggest that two genes, designated *CLAVATA1* (*CLV1*) and *SHOOT MERISTEMLESS* (*STM*), function in a competitive manner in the maintenance of indeterminate cells (Clark *et al*., 1996). *CLV1* has been shown to encode a receptor kinase, suggesting the involvement of a signal transduction pathway operating via extracellular ligands in the regulation of SAM activity (Clark *et al*., 1997). Further, *STM* has been shown to encode a *knotted1*-like homeodomain protein and to function in meristem maintenance (Long *et al*., 1996). Thus, genes involved in SAM activities are just beginning to be cloned and their function determined. However, the molecular mechanisms controlling these processes are still poorly understood.

Possible candidates for the genes involved in the various regulatory networks operative in SAM activities are homeobox genes, which encode an evolutionarily conserved 64 amino acid protein motif called homeodomain. Homeobox genes were first identified as homeotic genes in *Drosophila* and were subsequently cloned from other eukaryotic organisms including plants. In animals, homeobox genes are often involved as transcriptional factors in the pattern-forming and/or cell-specification events of embryogenesis that operate as master regulators of these processes (Manak and Scott, 1994).

The first higher plant homeobox gene to be cloned was *knotted1* (*kn1*) from the maize *Kn1* mutant (Vollbrecht *et al*., 1991). Leaf blades of the *Kn1* mutants exhibit sporadic outgrowths called knots along the lateral veins and ligule displacements. *Kn1* is a dominant mutation, caused by ectopic expression of *kn1* in leaves, that results in the disorganization of the developmental program of leaf blades (Smith and Hake, 1994). Many homeobox genes have subsequently been cloned from various plant species and, based on amino acid-sequence similarities within the homeodomain or conserved protein motifs outside of the homeodomain, these homeobox genes have been classified into five groups (Kerstetter *et al*., 1994; Lu *et al*., 1996). Of these, we focused on the *kn1*-type homeobox genes. Many *kn1*-type homeobox genes have been cloned from various plants and it is reported that they constitute a closely related small gene family within each plant species.

Recently, loss-of-function alleles of *kn1* were reported (Kerstetter *et al*., 1997). Although some of the phenotypes exhibited poor penetrance, perhaps due to genetic redundancy in maize, these mutations have revealed a role for *kn1* in meristem maintenance. In animals, families of related homeobox genes are often involved in related developmental processes (Gehring *et al*., 1994). Based on the observation that most of the *kn1*-type homeobox genes are expressed in the SAM (Smith *et al*., 1992; Jackson *et al*., 1994; Lincoln *et al*., 1994; Tamaoki *et al*., 1997), and from the phenotypes of the loss-of-function mutations in *kn1* and *STM* (Long *et al*., 1996; Kerstetter *et al*., 1997), it is believed that genes of this class are involved in the maintenance of the SAM and/or the development of lateral organs from the SAM, although the biological event(s) in which each *kn1*-type homeobox genes is engaged is still unclear except for *kn1* and *STM*.

The *kn1*-type homeobox genes often cause severe morphological abnormalities when overexpressed in tobacco, *Arabidopsis* and tomato, and in dominant mutations in maize, barley, or tomato (Matsuoka *et al*., 1993; Sinha *et al*., 1993; Smith and Hake, 1994; Müller

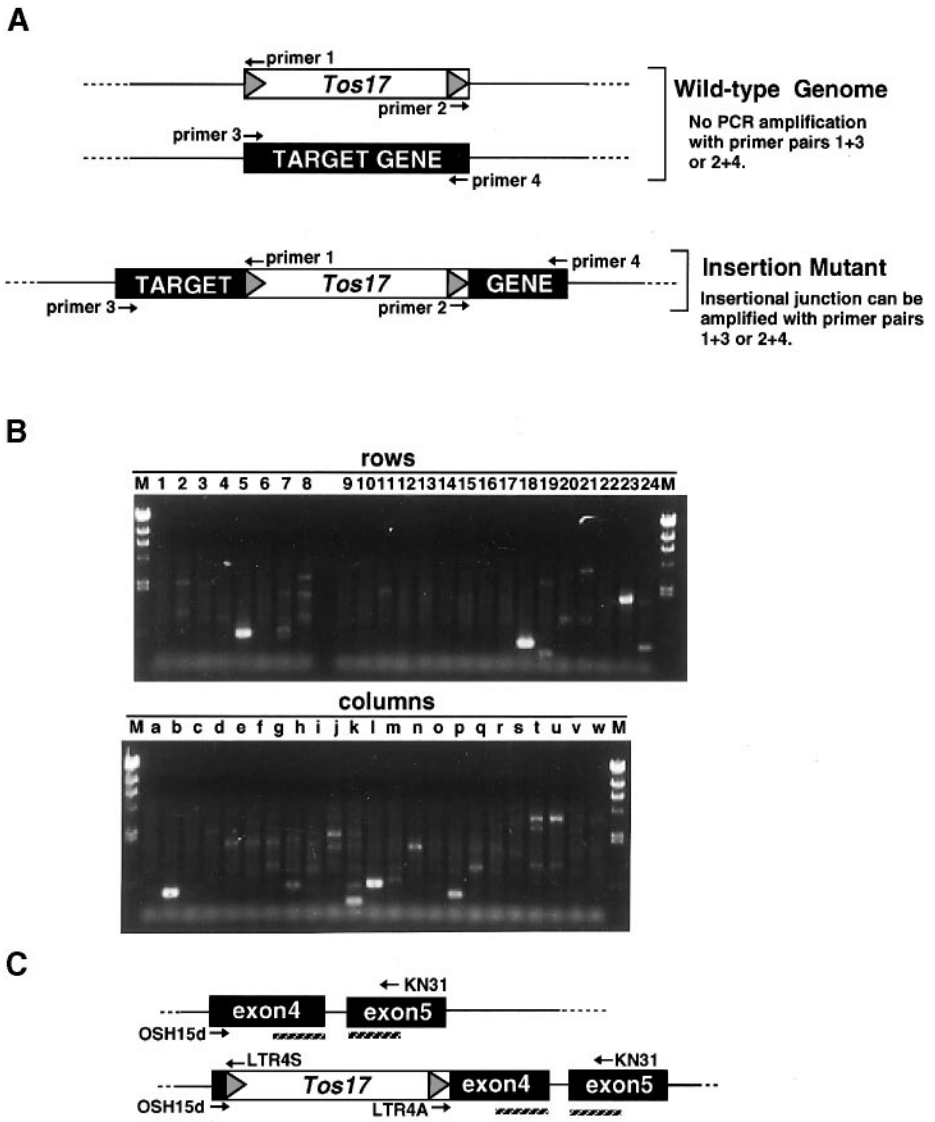

Fig. 1. (**A**) Methodology for detecting transposon insertions. An insertion of the rice retrotransposon *Tos17* into a target gene can be detected by PCR amplification using primer pairs 1+3 or 2+4. Triangles indicate the LTR. (**B**) Detection of transposon insertions into a rice homeobox gene. DNA from ~550 plants was amplified by PCR using LTR4S and KN31 as primers. A two-dimensional pool sampling system enabled the testing of ~550 plants in only 47 PCRs. The number or letter of each pooled DNA sample is shown at the top of the figure. M: DNA digested with *Hin*dIII. (**C**) Insertion site of the rice retrotransposon *Tos17* into the fourth exon of the rice homeobox gene *OSH15*. Filled boxes indicate exons and bold underlining indicates the approximate position of the homeodomain. The length of *Tos17* is not drawn to scale; *Tos17* is 4.3 kbp whereas the homeodomain is 190 bp.

et al., 1995; Schneeberger *et al*., 1995; Chuck *et al*., 1996; Hareven *et al*., 1996; Chen *et al*., 1997; Tamaoki *et al*., 1997). However, it is difficult to determine the function(s) of these genes in the wild-type context from the phenotype of gain-of-function transgenic plants or dominant neomorphic mutations.

Rice has become a model plant for the study of monocotyledonous plants because of the feasibility of transformation, its relatively small genome size, the high saturation of molecular markers on the rice genome and the large-scale analysis of expressed sequence tags (Izawa and Shimamoto, 1996). Furthermore, the gene knock-out system using a rice retrotransposon, *Tos17*, has been recently exploited (Hirochika *et al*., 1996; Hirochika, 1997; H.Hirochika, in preparation). Transpositions of *Tos17* are activated during tissue culture and several copies of *Tos17* can be inserted into the rice genome. In this system, it is possible to screen for mutants by insertion of *Tos17* into genes of interest from a large pool of plants regenerated after a few months of tissue culture.

To gain an understanding of the genetic programs mediated by the action of the *kn1*-type homeobox genes in the SAM, we have isolated six homeobox genes grouped into the class1-type of the *kn1*-like homeobox gene family from rice. Most of these genes are expressed in or adjacent to the SAM and their expression patterns suggest that these genes may play a role in the maintenance of the SAM and/or differentiation of organs from the SAM. A crucial step in determining the wild-type function(s) of the *kn1*-type homeobox genes from rice is the isolation of recessive alleles. We report here on the isolation and characterization of loss-of-function mutants of the rice homeobox gene *OSH15* (*Oryza sativa* homeobox). We have analyzed the phenotype of plants carrying loss-of-

function mutations in *OSH15* and demonstrate a novel function of the *kn1*-like homeobox gene other than SAM formation and/or maintenance.

Results

Screening for loss-of-function mutations in the rice homeobox genes

Rare insertions of a transposable element into a gene can be detected by PCR-based screening (Ballinger and Benzer, 1989; Kaiser and Goodwin, 1990). If an insertion of a transposable element occurs in the gene of interest, a suitable template will be generated that can be amplified exponentially by PCR using gene-specific and transposon-specific primers. The methodology for screening for loss-of-function mutations in the rice homeobox gene is described in the legend to Figure 1A. We designed transposon-specific primers from the long terminal repeat (LTR) of *Tos17* in sense (LTR4S) and antisense (LTR4A) orientations and a gene-specific primer (KN31) from the conserved region of the *kn1*-type homeodomain. We performed PCR-based screening using either LTR4S or LTR4A plus KN31. For efficient screening, we adopted a pool sampling system in which plants were arranged in a two-dimensional matrix. Genomic DNA was isolated from leaves sampled in pools consisting of either a column or a row. In this way, the genomic DNA from each plant is represented in a unique combination of a row and a column. We screened 47 DNA pools consisting of 24 columns and 23 rows. These pools contained genomic DNA from ~550 plants in which transposition of the rice retrotransposon *Tos17* had been induced for a few months of tissue culture and random insertion had occurred. A range of amplification products was obtained (Figure 1B).

From these amplification products, discrete bands with the same size in a column and row were cloned and sequenced. DNA sequencing analysis revealed that the amplified DNA fragment derived from the pooled genomic DNA corresponding to column l and row 5 contained the sequences of *Tos17* and the rice homeobox gene *OSH15*, which belongs to the class1-type of the *kn1*-like homeobox genes. Since *Tos17* was inserted into the fourth exon of *OSH15*, just upstream of the homeodomain region (Figure 1C), this transposon-tagged gene was predicted to be a loss-of-function allele.

To confirm that the insertion of *Tos17* had occurred in the *OSH15* gene and was transmitted germinally, we performed genomic Southern blot analysis with individuals of the progeny of this plant. Genomic DNA was isolated, digested with *Xho*I and hybridized with a probe specific for *OSH15* (Figure 2A). Among 40 individual plants tested, three patterns of hybridizing bands were observed. These were a single 6.4 kbp band, two bands of 6.4 and 4.5 kbp or a single 4.5 kbp band. The number of individuals showing each pattern was 9, 21 and 10, respectively. The ratio of these numbers fits the theoretical 1:2:1 predicted for Mendelian inheritance. In the wild-type, only a band of 6.4 kbp in size was observed, as expected from a restriction map of the *OSH15* genomic clone which we isolated previously (see Figure 5B). Alternatively, a band of 4.5 kbp was predicted to be generated from the insertion allele of *OSH15* based on the restriction maps of *OSH15* and *Tos17*. Consequently, individuals showing a single band of 4.5 kbp were homozygous (–/–) for the insertion, those with two bands of 4.5 and 6.4 kbp were heterozygous (+/–) and those with a single band of 6.4 kbp were wild type (+/+). These observations confirmed that the insertion of *Tos17* had occurred in *OSH15* and was transmitted germinally.

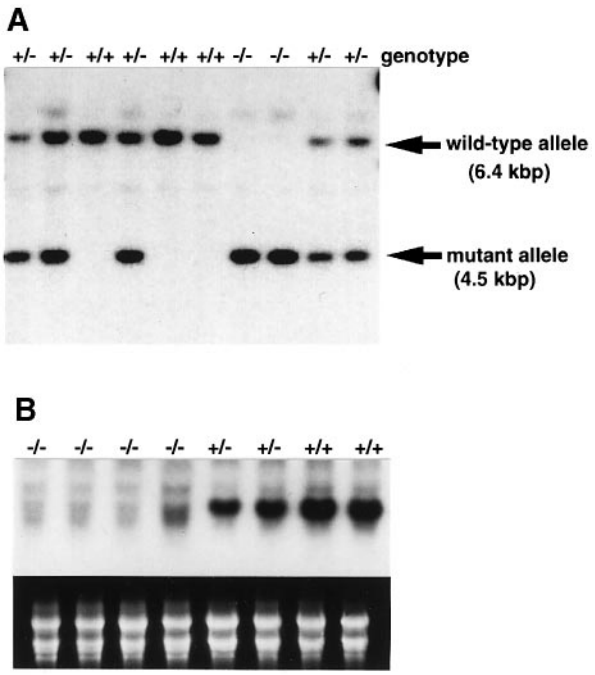

Fig. 2. (**A**) Cosegregation analysis by genomic Southern blot hybridization. Each lane contains 1 μg of genomic DNA digested with *Xho*I. In wild-type plants, a single 6.4 kbp band was detected (lanes +/+). A 4.5 kbp band was predicted, based on restriction maps of *Tos17* and *OSH15*, to be detected in *Xho*I digests containing the mutant allele. Therefore, individuals with only a single band at 4.5 kbp represent homozygotes (–/–) for the insertion and those showing bands at 6.4 and 4.5 kbp represent heterozygotes (+/–). (**B**) Northern blot analysis of RNA from the rachis of homozygous, heterozygous and wild-type (+/+) plants. A single band at 1600 nucleotides, corresponding to *OSH15* transcripts, was detected in heterozygous and wild-type plants but not in homozygous plants. The lower panel shows ethidium bromide-stained RNA corresponding to the above lanes to illustrate RNA loading levels.

To ensure that no normal *OSH15* transcript was generated from the mutant allele, total RNA was isolated from the rachis and subjected to Northern blot analysis. As shown in Figure 2B, no transcript was detected in the homozygous plants. This also suggests that the *Tos17* insertion represents a loss-of-function allele. Although signals corresponding to the *OSH15* transcript were detected in both wild-type and heterozygous plants, the intensity of the signal in wild-type plants was about twice as strong as that in heterozygotes (Figure 2B). Thus, the expression level of *OSH15* was controlled in a dose-dependent manner.

Next we observed the phenotype caused by loss-of-function of *OSH15*. Among 112 plants examined, no abnormality in morphology was observed in plants heterozygous for the insertion (59 individuals) or wild-type plants (27 individuals) under normal growing conditions, whereas all the plants homozygous for the insertion (26 individuals) displayed a dwarf phenotype (Figure 3A), indicating that the insertion of *Tos17* into *OSH15* was genetically linked to the dwarf phenotype.

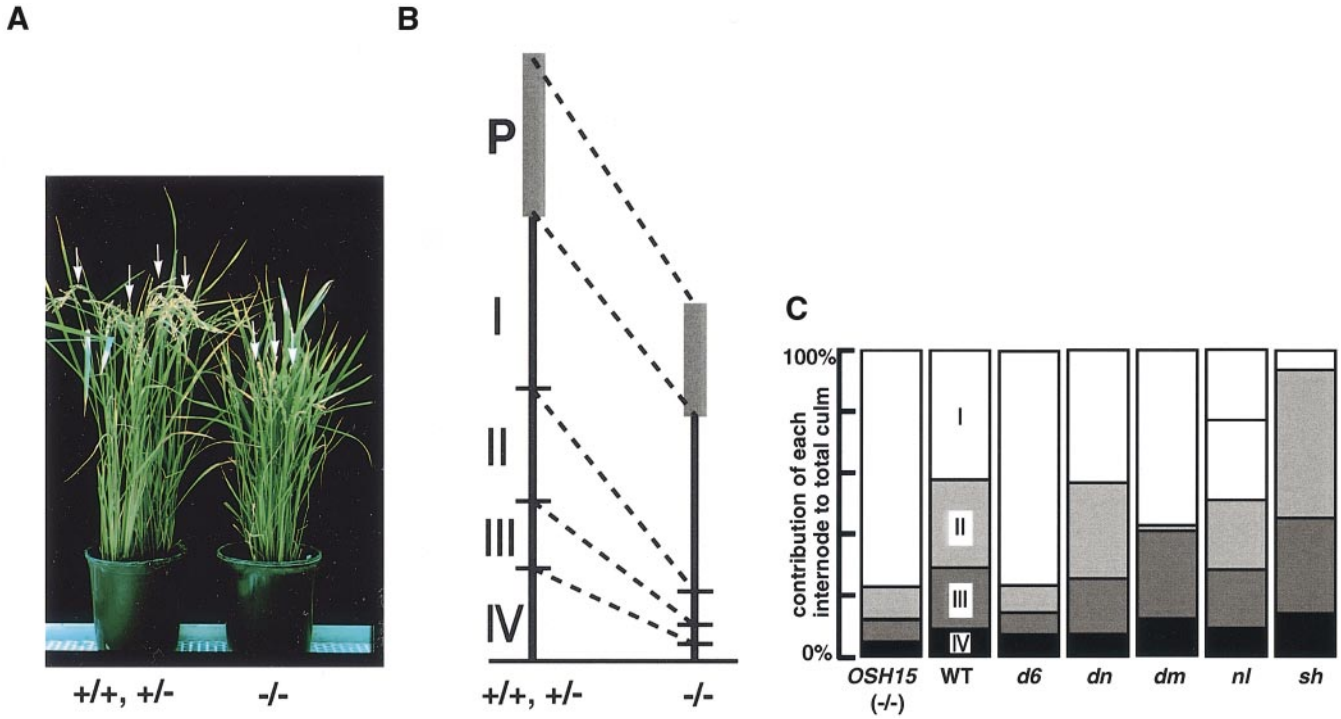

Fig. 3. (**A**) The appearance of homozygous (–/–), heterozygous (+/–) and wild-type (+/+) plants. All homozygous plants exhibited a dwarf phenotype (compare the height of the positions of the panicles, which are indicated by white arrows). (**B**) Comparison of the length of panicles and the upper four internodes of homozygous, heterozygous and wild-type plants. The lengths of panicles and the upper four internodes of 10 main culms were averaged in each genotype. In mutants, the lengths of the second, third and fourth internodes were severely reduced. (**C**) Schematic representation of internode elongation patterns of various dwarf mutants of rice (redrawn from Takeda, 1977). The internode elongation pattern of *OSH15* (–/–) plants were integrated into this panel based on the data on the relative contributions of each internode to total culm shown in Table I.

Identification of additional mutant alleles of OSH15

To confirm that the dwarf phenotype was caused by the loss of *OSH15*, we sought additional mutant alleles of *OSH15*. Because of their agronomic importance, a large number of dwarf mutants of rice have been isolated and characterized. These mutants are categorized into six groups based on the elongation pattern of the upper four to five internodes (Figure 3C; redrawn from Takeda, 1977). In this diagram, the relative length of each internode to total culm is drawn schematically. In rice, each internode is numbered from top to bottom such that the uppermost internode is first. In the *dn*-type mutant, the length of each internode is uniformly reduced resulting in an internode elongation pattern very similar to that of the wild-type. In contrast, the *dm*-type mutant shows specific reduction of the second internode. Shortening of a specific internode is also observed in the *sh*-type mutant, in which only the first (uppermost) internode is shortened. In the *d6*-type mutant, internodes below the uppermost are shortened. In the *nl*-type mutant, the fourth internode is relatively longer but the first internode is truncated.

In order to fit the *OSH15* loss-of-function mutant into this classification scheme of rice dwarf mutants, we measured the length of the upper four internodes and the panicle of the loss-of-function mutants and compared them with those of wild-type and heterozygous plants (Table I; Figure 3B). Although almost no difference was observed in the length of the panicle and the first (uppermost) internode between the mutant and the wild-type or heterozygous plant, the lengths of the second, third and fourth internodes in the mutant were shortened to ~25, 27 and 15% of the wild-type or heterozygote, respectively. By comparing this internode elongation pattern with the previously described six groups of dwarf mutants, we confirmed that the *OSH15* loss-of-function mutants clearly fit into the *d6*-type of dwarf mutants (Figure 3C).

Mutations at two different loci result in a *d6* phenotype (H.Kitano, unpublished results). Three alleles designated *d6-1*, *d6-ID6* and *d6-tankanshirasasa* (Nagao and Takahashi, 1963; Kinoshita and Shinbashi, 1982) have been identified at the *D6* locus, which maps to the telomere of the short arm of chromosome 7. All of these mutants are recessive and are often used as tester lines for this chromosome. *OSH15* also maps to a position 8.3 cM from the telomere end of the short arm of chromosome 7 (data not shown).

In order to test the possibility that the *d6* dwarf mutants are due to alterations of *OSH15*, we performed Southern blot analysis (Figure 4A). Genomic DNA was extracted from *d6-tankanshirasasa* (lane 1), *d6-1* (lane 2), *d6-ID6* (lane 3) and from two different wild-type cultivars, Taichung-65 (a parental line of *d6-1*, lane 4) and Shiokari (a parental line of *d6-ID6*, lane 5). These samples were digested with either *Sac*I or *Xho*I and hybridized with an *OSH15*-specific probe consisting of all of exon 4 and part of exon 5. In genomic DNA from wild-type plants digested with *Sac*I or *Xho*I, two bands of 4.5 and 5.0 kbp or a single band of 6.4 kbp were observed, respectively (Figure 4A, lanes 4 and 5). In contrast, no hybridizing bands were observed in genomic DNA from *d6-tankanshirasasa* or *d6-1* digested with either enzyme (Figure 4A, lanes 1 and 2). Similarly, no hybridizing bands were detected when the 5′ region upstream of *OSH15* was used to probe DNA

Table I. Length of each internode and relative contribution of each internode to the total culm length[a]

Genotype of *OSH15*	Length (cm) +/+	Length (cm) +/–	Length (cm) –/–
P	18.5 ± 0.7	18.4 ± 1.0	12.1 ± 0.8
I	26.8 ± 0.6 (40.1)	26.6 ± 0.9 (39.8)	23.8 ± 1.8 (71.5)
II	17.1 ± 1.4 (25.6)	17.1 ± 0.9 (25.6)	4.3 ± 0.8 (12.9)
III	13.9 ± 1.7 (20.8)	14.4 ± 0.3 (21.5)	3.8 ± 0.2 (11.4)
IV	9.0 ± 2.3 (13.5)	8.8 ± 2.0 (13.2)	1.4 ± 0.2 (4.2)

[a]Length of the upper four internodes and panicles of 10 main culms were measured and averaged in each genotype ($n = 10$). The relative contributions of each internode to the total culm length were calculated as percentages (numbers in parenthesis). The schematic view of the internode elongation pattern in Figure 3C was drawn by fitting the percentage data into the scheme as shown in Takeda (1977). In rice, it is usual for each internode to be numbered from top to bottom such that the uppermost internode is the first. P, panicle; I, uppermost internode; II, second internode; III, third internode; IV, fourth internode.

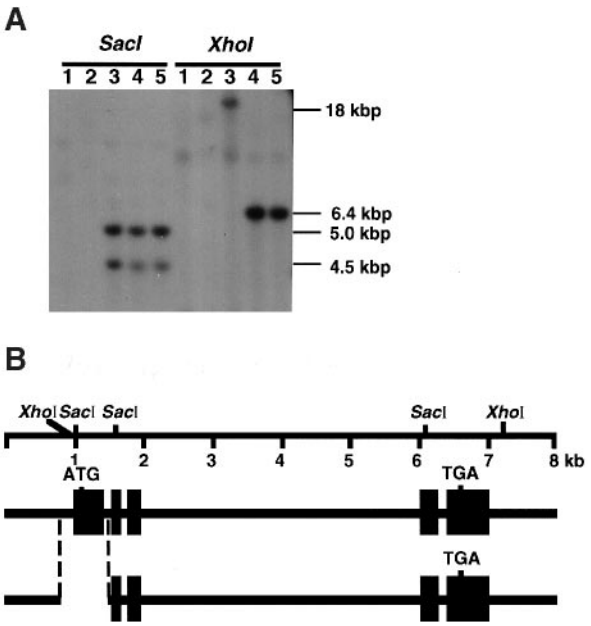

Fig. 4. (**A**) Detection of mutations in the *OSH15* genes of the three *d6*-type mutants by genomic Southern analysis. Each lane contains 1 μg of genomic DNA digested with either *Sac*I or *Xho*I. Numbers in the right indicate the approximate sizes of the specific bands. Lanes 1, *d6-tankanshirasasa*; lanes 2, *d6-1*; lanes 3, *d6-ID6*; lanes 4, Taichung-65; lanes 5, Shiokari. (**B**) Genomic structure around the *OSH15* gene in wild-type and *d6*-ID6. Boxes and bold lines indicate exons and introns plus untranslated regions, respectively. *Sac*I and *Xho*I restriction sites are indicated at the top. ATG and TGA indicate the position of the start and stop codons, respectively.

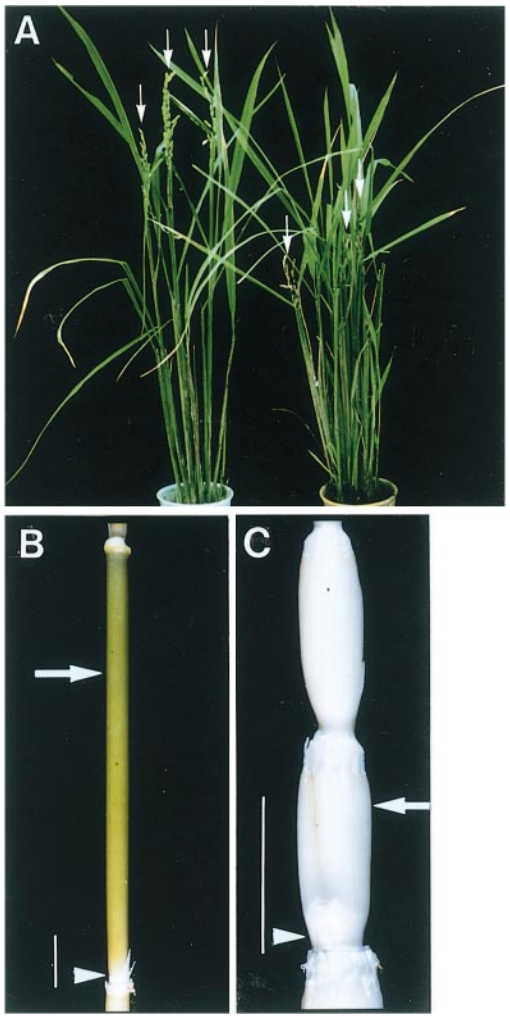

Fig. 5. (**A**) Complementation analysis of the *d6* phenotype. A 14 kbp wild-type genomic DNA fragment containing the entire 8 kbp *OSH15* coding region (plus introns) and 6 kbp of upstream DNA was used to transform *d6-1* dwarf rice mutants (left plant). As a control, the vector without the insert was also introduced (right plant). The normal phenotype was clearly restored in plants transformed with the *OSH15* gene (compare the height of the positions of the panicles, which are indicated by white arrows). (B–C) The appearance of internodes of wild-type and *d6* mutant plants. Side views of the fourth internode of a wild-type plant (**B**) and the third and fourth internodes of a *d6* dwarf mutant (**C**). Arrows indicate the approximate positions of cross sections shown in Figure 6C, D, E, F, G and H and arrowheads indicate the approximate positions of cross sections shown in Figure 6A and B. Bar = 1 cm.

from the dwarf mutants, whereas a specific band was detected in wild-type DNA (data not shown). Control hybridization experiments confirmed that the DNA was properly blotted onto the membrane in all lanes (data not shown). This indicates that, in *d6-tankanshirasasa* and *d6-1*, a deletion occurred in the region of the *OSH15* gene. In the case of *d6-ID6*, hybridizing bands of the same size as those of wild-type plants were observed in *Sac*I-digested genomic DNA (Figure 4A, left panel, lanes 3, 4 and 5). However, in *Xho*I-digested genomic DNA, a novel band of ~18 kbp was detected. This contrasts with the 6.4 kbp band detected in genomic DNA from wild-type plants (Figure 4A, right panel, lanes 3, 4 and 5). To identify the mutation in *d6-ID6*, we cloned and sequenced its entire coding region and the junctions of exons and introns. By comparing the sequences of the *d6-ID6* to its parental line, Shiokari, we determined that a deletion of ~700 bp including the entire first exon, the 5′ upstream region and part of the first intron had occurred (Figure 4B). As an *Xho*I site exists in the first exon of the wild-type gene, the *Xho*I-digested genomic DNA from *d6-ID6* showed a polymorphism compared with that from wild-type plants. Thus, all of the alleles of the *d6* locus contained deletions in the *OSH15* gene. This strongly

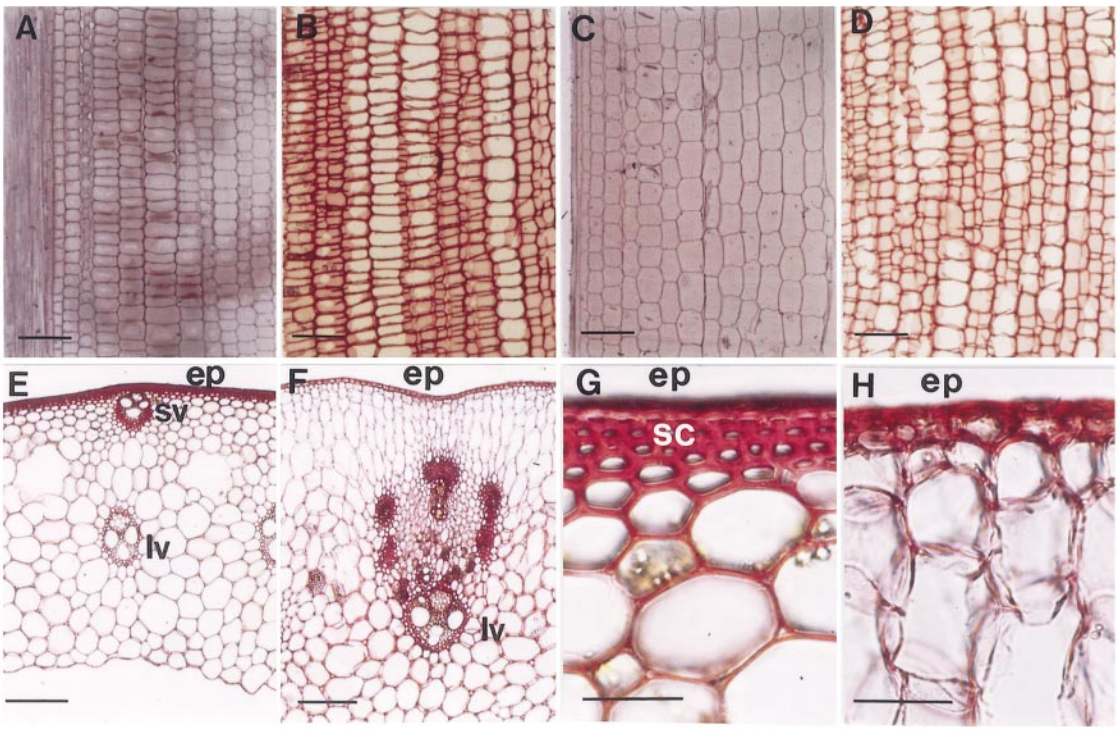

Fig. 6. Sections of the fourth internodes of wild-type and *d6* dwarf mutant plants. (**A**) Longitudinal section through the IM of the fourth internode of a wild-type plant. Bar = 100 μm. (**B**) Longitudinal section through the IM of the fourth internode of a *d6* mutant plant. Bar = 100 μm. (**C**) Longitudinal section through the elongated zone of the fourth internode of a wild-type plant. Bar = 100 μm. (**D**) Longitudinal section through the elongated zone of the fourth internode of a *d6* mutant plant. Bar = 100 μm. (**E**) Cross sections of the fourth internodes of wild-type. Bar = 100 μm. (**F**) Cross sections of the fourth internodes of *d6*. Bar = 100 μm. (**G**) Higher magnification of (E). Bar = 30 μm. (**H**) Higher magnifications of (F). Bar = 30 μm. Note that sections in panel (A) and (C) were stained with hematoxylin and the rest of sections were stained with safranin. ep, epidermis; sc, sclerenchymatous cell layers; sv, small vascular bundles; lv, large vascular bundles.

suggests that loss-of-function of the *OSH15* gene causes the *d6*-type dwarf phenotype in rice.

Molecular complementation analysis of d6 by OSH15

Next, we carried out complementation analysis of *d6-1* by the introduction of the wild-type *OSH15* gene. When we introduced a control vector that carries no rice genomic DNA to *d6-1*, no change in the culm length was observed (Figure 5A, right). However, when a 14 kbp DNA fragment containing the entire wild-type *OSH15* gene was introduced, the normal phenotype was recovered in three plants among 25 transgenic lines (Figure 5A, left), confirming that the *d6* dwarf mutant is caused by the loss-of-function mutation in the *OSH15* gene. The rest of the 22 transgenic lines showed the abnormal leaf morphology and short stature that was observed in the overexpression of *OSH15* in rice (Y.Sato and M.Matsuoka, unpublished results). This was probably due to the ectopic expression of *OSH15* caused by multiple insertions of the transgene.

Anatomy of the d6 mutant internode

In order to clarify how *OSH15* functions in internode elongation, we carried out an examination of the anatomy of the internode architecture of the *d6* mutant. In wild-type rice plants, concomitant with the change from vegetative to reproductive growth, the upper four to six internodes start to elongate in succession from base to top. When an internode elongates, the intercalary meristem (IM) differentiates at the base of the internode. Internode elongation is caused by mitotic activity in cells in the IM and by the elongation of these cells in the elongation zone immediately above the IM.

Figure 5B and C shows the mature fourth internode of a wild-type plant and the third and fourth internodes of a *d6-1* mutant. Although the differentiation of nodes and internodes is obvious in both cases, internode elongation was severely disturbed in the *d6-1* mutant.

In order to understand the cellular basis of the *d6* mutant internode phenotype, we prepared sections of internodes from the wild-type and mutant plants and observed them microscopically. In longitudinal sections of wild-type mature fourth internodes at 2–3 mm above the node, cells in IM were observed to be closely packed and small sized (Figure 6A). Similar results were obtained with the *d6* mutant (Figure 6B), demonstrating that differentiation of the IM was not affected in the *d6* mutant. In the upper region of the internode in the wild-type plants, parenchyma cells elongated longitudinally up to ~120 μm in length (Figure 6C). However, in the *d6* mutant, the size of the parenchyma cells reached up to ~60 μm, and thus the parenchyma cell elongation was less evident than that in the wild-type (Figure 6D). The reduction in the cell size in the *d6* mutants was also observed in the second and third internodes, as well as in the fourth internode; in the uppermost internode, no reduction in cell size was observed in the mutants (data not shown).

In the elongated region of internodes in the wild-type, epidermal cells and hypodermal sclerenchymatous cell layers were observed in the outer part of the stem. Hypodermal sclerenchymatous cells in the wild-type plants were very long (often reaching 1 mm in length) and

slender and had well developed secondary cell walls (Figure 6E and G). Fourteen or fifteen small vascular bundles were arranged concentrically in the inside of the sclerenchymatous cell layer. Large vascular bundles were also arranged concentrically in the inner region and air spaces were located between them.

In *d6-1*, the organization of small vascular bundles was severely disrupted whereas the arrangement of large vascular bundles was similar to that seen in wild-type plants (Figure 6F). In addition, epidermal cells of mutant internodes were obviously enlarged and hypodermal sclerenchymatous cells, characterized by well developed secondary walls, were absent. Instead, in place of hypodermal cells, vacuolated cells resembling parenchyma cells were observed (compare Figure 6G and H). The number of cell layers from the epidermis to the air spaces (8–9 layers) or to the large vascular bundles (13–15 layers) constituting the outer part of an internode were similar in the wild-type and mutant internodes. These observations suggest that the radial pattern was not affected, but that the differentiation of hypodermal sclerenchymatous cell layers was defective in *d6-1* internodes.

Epidermal cell shape was observed in sections taken parallel to the epidermis using Nomarski optics. In the wild-type internodes, long rectangular cells with a wavy margin, termed long cells, were observed. The long cells were interrupted by pairs of oval cells, termed silica and cork cells, which derived from a single cell termed a short cell (Figure 7A and B). In internodes of the *d6-1* allele, the epidermal architecture was quite different from that in the wild-type. We observed large, distorted cells with smooth margins that probably corresponded to the long cells in the wild-type. In addition, small cells were frequently seen which probably corresponded to short cells. However, the differentiation of silica and cork cells was rarely observed (Figure 7C and D). These epidermal phenotypes are specific to the *d6* mutant. Epidermal cells of other dwarf mutants defective in internode elongation, such as *d18* or *d1*, did not show these phenotypes (data not shown). Therefore, such modified epidermal architecture is not caused by the defect in internode elongation but rather may cause it (see Discussion).

We also observed the internode architecture of the first (uppermost) internode, rachis and pedicel from the wild-type plants and the *d6* mutant, the length of which were similar in both plants. In the cross section of the uppermost internode from wild-type plants, small and large vascular bundles and hypodermal sclerenchymatous cells with well developed secondary cell walls were observed (Figure 8A and B). It was a specific feature of the uppermost internode that small vascular bundles protruded to the outer part of the stem. In the *d6* mutants, the development of hypodermal sclerenchymatous cells was not observed and instead, parenchyma-like cells were observed as in the unelongated internodes below the uppermost (Figure 8D and E). Similar abnormal development of hypodermal cells was also observed in the stem portion of the rachis and the pedicel (Figure 8C and F; and data not shown). In contrast with the abnormal hypodermal cells in the uppermost internode, rachis and pedicel of *d6* mutants, the small vascular bundles and the epidermal cell shape were normal and the size of the parenchyma cells were almost the same in length between the wild-type and the mutant in these organs (Figure 8D and G; data not shown).

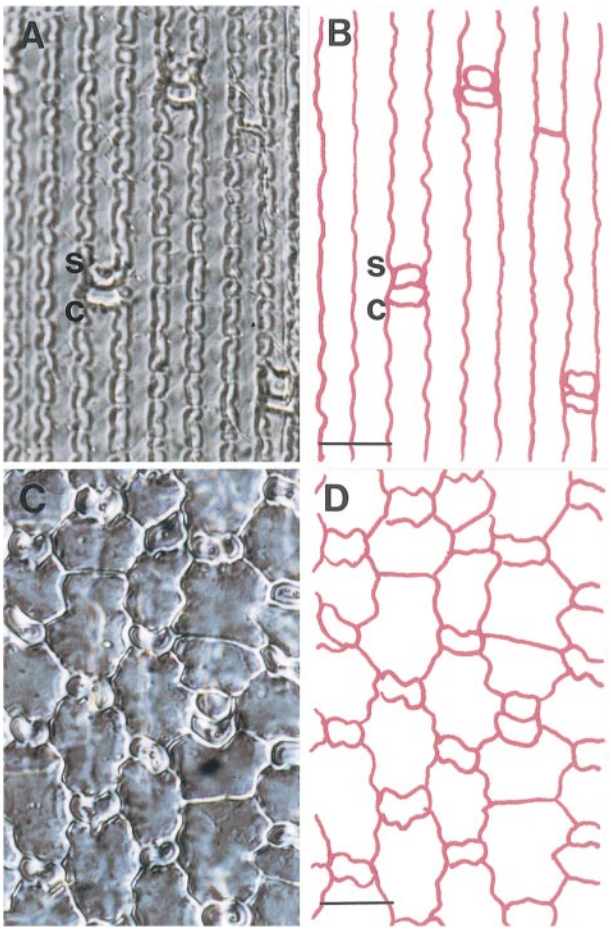

Fig. 7. Epidermal cell configuration of the fourth internode in the wild-type and *d6* mutant. (**A** and **B**) wild-type; (**C** and **D**) *d6*. Bar = 20 μm. s, silica cell; c, cork cell.

Expression pattern of the OSH15 gene

Since the loss-of-function mutation of *OSH15* affects the development of epidermal and hypodermal cells, we predicted that the expression of *OSH15* may be restricted to the outer cells of the differentiating internode. To address this possibility, we performed *in situ* hybridization to observe the localization of *OSH15* mRNA. In longitudinal sections, *OSH15* expression was localized just below the leaf insertion points and at the primordia of axillary buds (Figure 9A). In cross sections through planes of leaf insertions, *OSH15* mRNAs were observed in a ring-shaped pattern (Figure 9B, C and D). This localized expression of *OSH15* corresponds well to the pattern of phenotypic defects observed in the loss-of-function mutants.

Discussion

Targeted inactivation of the rice homeobox gene OSH15

To gain an understanding of the biological function of rice homeobox genes, we screened for loss-of-function mutants. We identified one such mutation in *OSH15* from ~550 plants that were mutagenized by the random

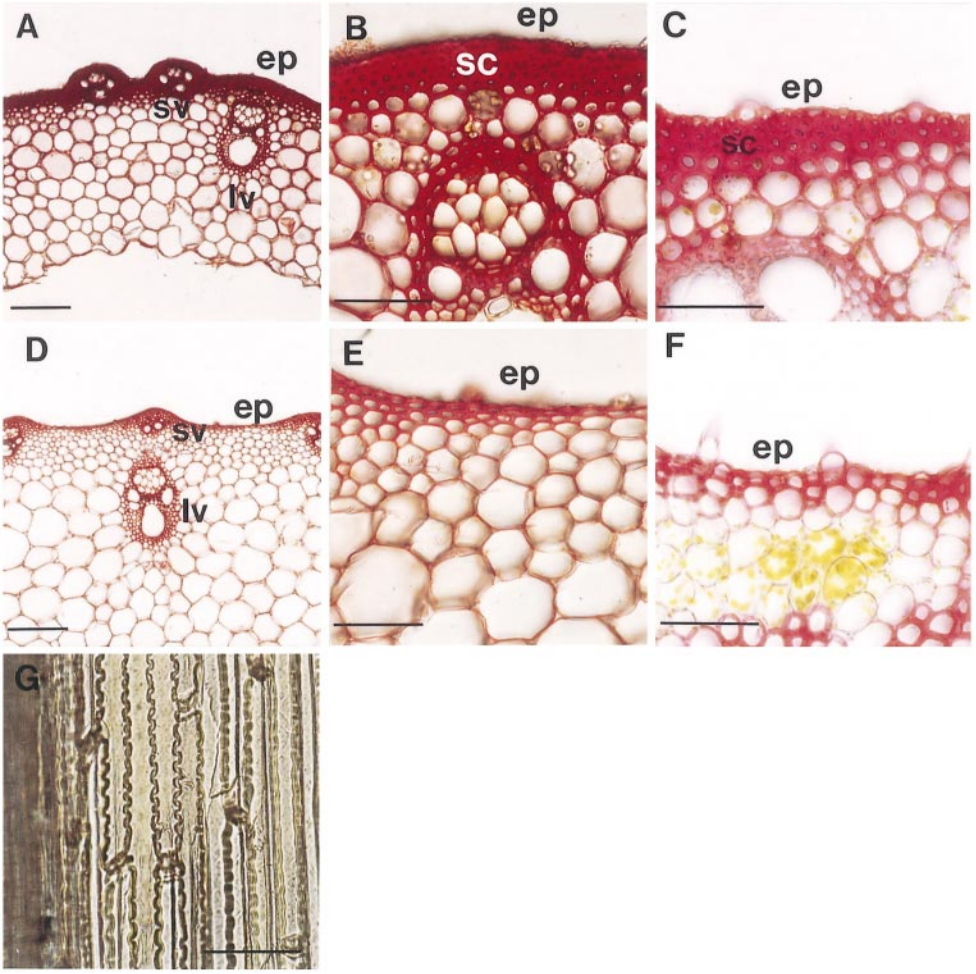

Fig. 8. Sections of the uppermost internodes and rachis of wild-type and *d6* dwarf mutant plants. (**A**) Cross section of the uppermost internode from a wild-type plant. Bar = 100 μm. (**B**) Higher magnifications of (A). Bar = 30 μm. (**C**) Cross section of the rachis from a wild-type plant. Bar = 30 μm. (**D**) Cross section of the uppermost internode from a *d6* mutant plant. Bar = 100 μm. (**E**) Higher magnifications of (D). Bar = 30 μm. (**F**) Cross sections of the rachis from a *d6* mutant plant. Bar = 30 μm. (**G**) Epidermal cell configuration of the uppermost internode in the *d6* mutant plant. Bar = 30 μm. ep, epidermis; sc, sclerenchymatous cell layers; sv, small vascular bundles; lv, large vascular bundles.

insertions of the rice retrotransposon, *Tos17*. Considering the number of mutagenized rice lines screened and the number of *Tos17* insertions per mutagenized line (5–30; Hirochika *et al*., 1996), the knock-out line of *OSH15* should have been isolated by chance. In order to make the gene knock-out system generally applicable to any gene, insertion mutations induced by *Tos17* should be saturated. In order to achieve this, a large number of mutagenized lines are being produced (Hirochika, 1997).

All the plants homozygous for the insertion of *Tos17* into the *OSH15* gene showed a dwarf phenotype with properties similar to the conventional dwarf mutants, *d6*. From the following data we conclude that this dwarf phenotype was caused by the loss-of-function of *OSH15*. First, all conventional *d6* mutants have complete or partial deletions in the *OSH15* gene that caused its loss-of-function. Secondly, the *d6* dwarf phenotype was complemented by the introduction of a wild-type *OSH15* gene.

The *OSH15* gene in rice encodes a member of the *kn1*-type of the homeobox transcription factors (Sato *et al*., 1998). Homeobox genes encode a highly conserved protein motif, the homeodomain, which acts as a sequence-specific DNA binding motif (Gehring, 1992). Based on the deduced amino acid sequence around the homeodomain of *OSH15*, this gene is classified into the class1-type of the *kn1*-like gene family. *OSH15* is most similar to maize *rs1* (*rough sheath1*) and *knox4* (Kerstetter *et al*., 1994) and its map position is 8.3 cM on rice chromosome 7, where synteny to the maize chromosome regions of both *rs1* and *knox4* is observed (Ahn and Tanksley, 1993). These results indicate that *OSH15* may be an ortholog of maize *rs1* and *knox4*. The presence of two *OSH15* orthologs in maize may be due to the genetic redundancy in this species (Helentjaris *et al*., 1988). It may be advantageous to find out the phenotype caused by a single gene mutation in rice, because of the lesser genetic redundancy in rice than maize.

Most class1-type genes of the *kn1*-like homeobox gene family are expressed around the SAM and thought to be involved in SAM formation and/or maintenance. Loss-of-function alleles have been identified in *kn1* from maize (Kerstetter *et al*., 1997) and *STM* from *Arabidopsis* (Long *et al*., 1996). In both of these mutants, defects related to SAM maintenance, such as abnormal branching pattern and lateral organ formation, or maintenance of the SAM in the embryo were observed. In a previously published paper on the expression profile of *OSH15* (Sato *et al*., 1998), we have reported that the expression pattern of

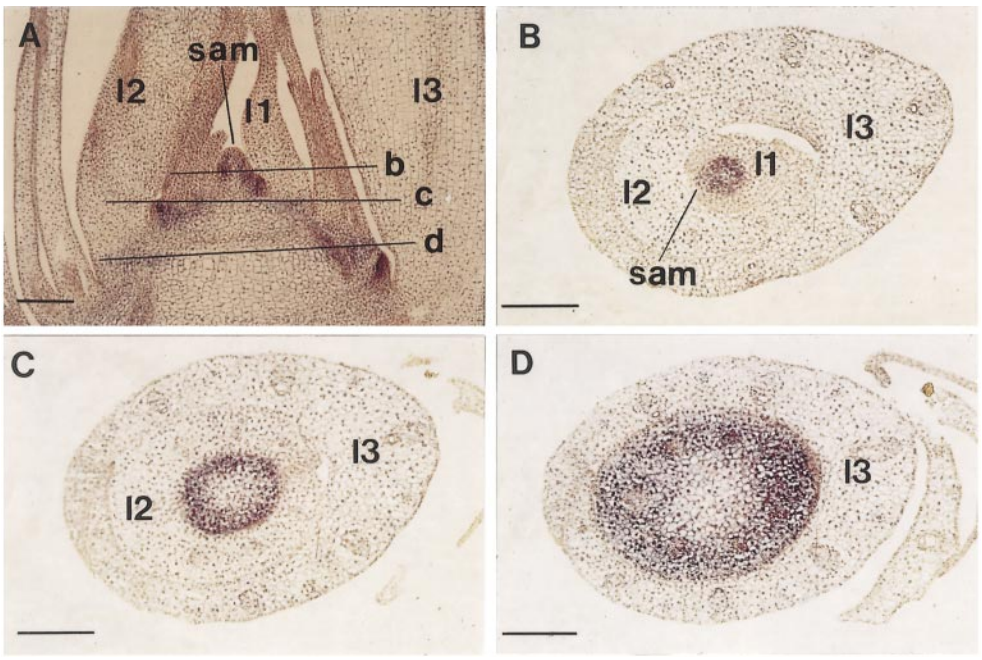

Fig. 9. *In situ* localization of *OSH15* mRNA in the rice vegetative shoot. (**A**) Longitudinal section of a rice vegetative shoot. Lines b, c and d indicate the plane of cross sections corresponding to (**B**), (**C**) and (**D**). Bar = 100 μm. sam, shoot apical meristem; leaves are indicated by 11, 12 and 13 in order of their youth.

OSH15 changes dramatically between the early embryogenesis stage and thereafter. Based on this observation, we have suggested that *OSH15* may play two different roles in plant development and, in the early embryogenesis, *OSH15* may be involved in SAM formation and/or maintenance, because it shows a similar expression pattern to *kn1*, *STM* and *OSH1* (Smith *et al*., 1995; Sato *et al*., 1996). In contrast with these previous observations, we could not identify any abnormality related to SAM formation or maintenance during early embryogenesis in the *OSH15* loss-of-function mutants (data not shown). This does not lead to the conclusion that *OSH15* is not related to SAM formation and/or maintenance at this stage, because the redundant gene(s) may compensate for this process in the early embryogenesis. This is supported by the fact that there are at least three additional *kn1*-type homeobox genes in rice that show similar expression pattern to *OSH1* and *OSH15* during early embryogenesis (N.Sentoku, Y.Sato and M.Matsuoka, unpublished data).

The role of OSH15 in the development of internode

We found that the loss-of-function mutations in *OSH15* resulted in a *d6*-type dwarf phenotype. In *d6* mutants, internodes below the uppermost are shortened. We observed several defects in these internodes. In the mutant internodes, obscurity of the vertical elongation of cells both in the parenchyma and the epidermis, disorganization of small vascular bundles, displacement of hypodermal sclerenchymatous cells to parenchyma-like cells and aberrant shapes of epidermal cells were observed (Figures 6–8). From observations of dwarf mutants unrelated to the *d6* mutation, it was suggested that abnormalities seen in the small vascular bundles, hypodermal sclerenchymatous cells and epidermal cells are not general characteristics of dwarf mutants but rather are specific to the *d6* mutants. Therefore, these abnormalities may be caused by the loss-of-function of *OSH15* and responsible for the defect in internode elongation in *d6* mutants.

Based on the phenotype of the loss-of-function mutants and the expression pattern of *OSH15*, we considered how *OSH15* may function in rice development. *OSH15* expression was observed just below the leaf insertion point around the SAM, where the internode would later develop, before any visible differentiation of the node or the internode is recognized (Figure 9). The *OSH15* mRNA is present in a ring-shaped pattern which delineates the several cell layers destined to become the outer part of the internode. The loss-of-function phenotypes that were specific to the *d6* mutant internodes were observed only in the outer part of the internodes. Taken together, these results indicate that *OSH15* may respond to the positional cues that specify the several outer cell layers of developing internodes and control the development of small vascular bundles, sclerenchyma and epidermal cells.

How could loss-of-function of *OSH15* change the morphology and/or differentiation of cells in these tissues? We hypothesized two possible models of actions of *OSH15*. One is that *OSH15* may affect the activity of IM through the regulation of the cell division rate in IM and/or the maintenance of meristematic activity of IM. In the lower internodes, the size of parenchyma cells were shortened to ~60 μm in length in the *d6* mutant, while in the wild-type the cell length was ~120 μm (Figure 6C and D; data not shown). Considering the fact that the length of the second, third and fourth internodes in the mutant was shortened to 25, 27 and 15%, respectively, the number of cells in each internode was calculated to be reduced to ~50, 54 and 30%, respectively, relative to the wild-type plants. The reduction of cell numbers per internode means that the frequency of cell division in IM is decreased, because almost all cells in internodes are derived from

IM. Thus, *OSH15* may have functions relating to the activity of IM. Defects in the normal morphogenesis and/or development of cells observed in the loss-of-function mutant of *OSH15* could be a consequence of a primary defect in cell division in IM. Indeed, it has been shown that the lack of phloem cells in the embryonic root of *Arabidopsis wooden leg* mutant is a consequence of the reduced number of cells (Scheres *et al*., 1995). In the uppermost internode, the compensation by the redundant gene(s) for the function of *OSH15* may lead to the restoration of the reduction in cell division and its indirect effects, except for the development of the hypodermal sclerenchyma. The failure of the development of the hypodermal sclerenchyma in the uppermost internode without the defect in the activity of IM indicates that *OSH15* is involved in the development of this tissue in the uppermost internode independently from the IM activity.

The second possibility is that *OSH15* may act as a developmental switch by which the hypodermal cells develop as sclerenchymatous cells. On this hypothesis, it is conceivable that, in the loss-of-function mutant, the development of sclerenchymatous cells was blocked and, instead, the cells developed into parenchyma-like cells. This possibility is also supported by the fact that the defect in the normal development of hypodermal sclerenchymatous cells is consistently observed even in the uppermost internode, rachis and pedicel of the *d6* mutant (Figure 8E and F), while these organs in the *d6* mutants exhibited otherwise almost normal development.

Since the uppermost internode, rachis and pedicel of the *d6* mutants developed normally except for the development of the hypodermal sclerenchyma, other defects observed in the second, third and fourth internodes could be interpreted as indirect effects of the abnormal development of the hypodermal sclerenchyma. Why these tissues fail to develop normally in the unelongated lower internodes of the *d6* mutant is explainable by the cell–cell interactions in these tissues and the adjacent hypodermal cells. In the uppermost internode, rachis and pedicel unknown factor(s) may compensate for this process, and consequently, these organs develop normally even in the absence of hypodermal sclerenchymatous cells.

Materials and methods

Plant growth conditions

Rice plants were grown in the field or in the greenhouse at 30°C (day) and 24°C (night). Rice dwarf mutants (*d6-1*, *d6-tankanshirasasa*, *d6-ID6*) were described in Kinoshita and Shinbashi (1982) and Nagao and Takahashi (1963).

PCR amplification and sequencing

For screening loss-of-function mutants, DNA fragments in which *Tos17* was inserted into the rice homeobox genes were amplified by PCR using transposon-specific primers designated LTR4S and LTR4A and a gene-specific primer designated KN31 from 300 ng of rice genomic DNA sampled from a pool of 23 or 24 plants. PCR products were gel purified and cloned into the pCRII vector (Invitrogen). Details of mutagenesis with *Tos17* and the pool sampling system will be described elsewhere (H.Hirochika, in preparation).

For sequencing of the entire coding region of *d6-ID6* and Shiokari, exon and exon/intron border sequences were amplified by PCR from 30 ng of rice genomic DNA using primers PF2-I2R, I2F-I3R and I3F-RR. To avoid PCR artifacts, we carried out three independent PCRs with each primer set. PCR products were gel purified and cloned separately into pCRII. Primer sequences were as follows. LTR4S: CTGGACATGGGCCAACTATACAGT; LTR4A: ACTGTATAGTTGGCCCATGTCCAG; KN31: CCGAATTCTGGTTGATGAACCAGTTGTT; PF2: ATCTTCAAACTTTAATTCCTCC; I2R: CATGAACGATATATGAACTGG; I2F: GGGTTGATTAATCGGAATCG; I3R: GGGGATGGATGATTGGTTG; I3F: AACATGGTCATGACTGAAGC; RR: AACATGATCGAGACCTTGTC. Nucleotide sequences were determined by the dideoxynucleotide chain-termination method using an automated sequencing system (ABI373A). Analysis of the nucleotide sequences was carried out using GENETYX computer software (Software Kaihatsu Co., Japan).

Genomic DNA isolation and Southern blot hybridization

Rice genomic DNA was isolated by ISOPLANT DNA isolation kit (Nippon GENE Co., Japan) from leaf tissue and 1 μg was digested with restriction enzymes, transferred onto Hybond N^+ membranes (Amersham) under alkaline conditions and analyzed by Southern hybridization. A cDNA probe specific for *OSH15*, which consisted of the fourth and part of the fifth exon, was amplified by PCR using the primers OSH15d (GATGGTAAATCTGAATGTG) and KN31. Hybridization was performed as described in Church and Gilbert (1984) except that membranes were hybridized at high stringency (68°C).

RNA isolation and Northern blot hybridization

Total RNA was isolated from rice rachis tissues by the method described by Chomczynski and Sacchi (1987) and 10 μg were electrophoresed in a 1% agarose gel, then transferred to a Hybond N^+ membrane (Amersham) and analyzed by Northern blot hybridization. The probe and hybridization conditions were the same as those used in the Southern analysis.

Complementation analysis

To construct pBI-OSH15, a restriction fragment covering the 14 kbp region of the *OSH15* genomic locus was cloned into the *Hin*dIII–*Sal*I site of the hygromycin resistant binary vector pBI101-Hm3. This vector was a modification of pBI-H1 (Ohta *et al*., 1990) and contains a unique *Bam*HI site in the multiple cloning site. pBI-cont, which was used as a control vector and contained no insert, was constructed from pBI101-Hm3 by digestion with *Sal*I and religation. Binary vectors were introduced into *Agrobacterium tumefaciens* strain EHA101 (Hood *et al*., 1986) by electroporation. Rice transformation was performed as described in Hiei *et al*. (1994).

Histological analysis

Plant materials were fixed in formalin:acetic acid (FAA):70% ethanol (1:1:18) embedded in ice on a cryostat, cut into 20 μm sections and stained with safranin. For hematoxylin staining, plant materials fixed in FAA were dehydrated through a graded ethanol series and embedded in Technovit 7100 resin (Kulzer & Co. GmbH, Wehrheim, Germany). Microtome sections (3–5 μm thick) were stained with hematoxylin.

In situ hybridization analysis

In situ hybridization with digoxigenin-labeled RNA, produced from the *OSH15* coding region without a poly(A) tail, was conducted as described previously (Kouchi and Hata, 1993). Tissues were fixed with 4% (w/v) paraformaldehyde and 0.25% glutaraldehyde in 0.1 M $NaPO_4$ buffer and embedded in Paraplast Plus. Microtome sections (7–10 μm thick) were applied to glass slides treated with Vectabond (Vector Laboratory). Hybridization and immunological detection of the hybridized probe were performed using the method described by Kouchi and Hata (1993).

Acknowledgements

We are grateful to Drs Masahiro Yano and Takuji Sasaki for mapping *OSH15* to rice genome and Dr Kenzo Nakamura for providing the vector for rice transformation. We thank Drs Sarah Hake, Yasuo Nagato and Keisuke Nemoto for their critical comments on the manuscript. This research was supported by a Grant-in-Aid for Scientific Research on Priority Areas (The Molecular Basis of Flexible Organ Plans in Plants) from the Ministry of Education, Science and Culture (Japan) and Special Coordination Funds for Promoting Science and Technology from the Science and Technology agency (Japan) to M.M. and H.H., and the special coordination funds for promoting science and technology in Japan, and the program for promotion of Basic Research Activities for Innovative Biosciences to H.H. and from Research fellowships of the Japan Society for the Promotion of Science for Young Scientists to Y.S.

References

Ahn,S. and Tanksley,S.D. (1993) Comparative linkage map of the rice and maize genomes. *Proc. Natl Acad. Sci. USA*, **90**, 7980–7984.

Ballinger,D.G. and Benzer,S. (1989) Targeted gene mutations in *Drosophila*. *Proc. Natl Acad. Sci. USA*, **86**, 9402–9406.

Chen,J.J., Janssen,B.J., Williams,A. and Sinha,N. (1997) A gene fusion at a homeobox locus: alterations in leaf shape and implications for morphological evolution. *Plant Cell*, **9**, 1289–1304.

Chomczynski,P. and Sacchi,N. (1987) Single-step method of RNA isolation by acid guanidium thiocyanate-phenol-chloroform extraction. *Anal. Biochem.*, **162**, 156–159.

Chuck,G., Lincoln,C. and Hake,S. (1996) *KNAT1* induces lobed leaves with ectopic meristems when overexpressed in *Arabidopsis*. *Plant Cell*, **8**, 1277–1289.

Church,G. and Gilbert,W. (1984) Genomic sequencing. *Proc. Natl Acad. Sci. USA*, **81**, 1991–1995.

Clark,S.E., Jacobsen,S.E., Levin,J.Z. and Meyerowitz,E.M. (1996) The *CLAVATA* and *SHOOT MERISTEMLESS* loci competitively regulate meristem activity in *Arabidopsis*. *Development*, **122**, 1567–1575.

Clark,S.E., Williams,R.W. and Meyerowitz,E.M. (1997) The *CLAVATA1* gene encodes a putative receptor kinase that controls shoot and floral meristem size in *Arabidopsis*. *Cell*, **89**, 575–585.

Gehring,W.J. (1992) The homeobox in perspective. *Trends Biochem. Sci.*, **17**, 277–280.

Gehring,W.J., Affolter,M. and Bürglin,T. (1994) Homeodomain proteins. *Annu. Rev. Biochem.*, **63**, 487–526.

Hareven,D., Gutfinger,T., Parnis,A., Eshed,Y. and Lifschitz,E. (1996) The making of a compound leaf: genetic manipulation of leaf architecture in tomato. *Cell*, **84**, 735–744.

Helentjaris,T., Weber,D. and Wright,S. (1988) Identification of the genomic locations of duplicate nucleotide sequences in maize by analysis of restriction fragment length polymorphisms. *Genetics*, **118**, 353–363.

Hiei,Y., Ohta,S., Komari,T. and Kumashiro,T. (1994) Efficient transformation of rice (*Oryza sativa* L.) mediated by *Agrobacterium* and sequence analysis of the boundaries of the T-DNA. *Plant J.*, **6**, 271–282.

Hirochika,H. (1997) Retrotransposons of rice: their regulation and use for genome analysis. *Plant Mol. Biol.*, **35**, 231–240.

Hirochika,H., Sugimoto,K., Otsuki,Y., Tsugawa,H. and Kanda,M. (1996) Retrotransposons of rice involved in mutations induced by tissue culture. *Proc. Natl Acad. Sci. USA*, **93**, 7783–7788.

Hood,E.E., Helmer,G.L., Fraley,R.T. and Chilton,M.-D. (1986) The hypervirulence of *Agrobacterium tumefaciens* A281 is encoded in a region of pTiBo542 outside of T-DNA. *J. Bacteriol.*, **168**, 1291–1301.

Izawa,T. and Shimamoto,K. (1996) Becoming a model plant: the importance of rice to plant science. *Trends Plant Sci.*, **1**, 95–99.

Jackson,D., Veit,B. and Hake,S. (1994) Expression of maize *KNOTTED1* related homeobox genes in the shoot apical meristem predicts patterns of morphogenesis in the vegetative shoot. *Development*, **120**, 405–413.

Kaiser,K. and Goodwin,S.F. (1990) 'Site-selected' transposon mutagenesis of *Drosophila*. *Proc. Natl Acad. Sci. USA*, **87**, 1686–1690.

Kerstetter,R., Vollbrecht,E., Lowe,B., Veit,B., Yamaguchi,J. and Hake,S. (1994) Sequence analysis and expression patterns divide the maize *knotted1*-like homeobox genes into two classes. *Plant Cell*, **6**, 1877–1887.

Kerstetter,R.A., Laudencia-Chingcuanco,D., Smith,L.G. and Hake,S. (1997) Loss-of-function mutations in the maize homeobox gene, *knotted1*, are defective in shoot meristem maintenance. *Development*, **124**, 3045–3054.

Kinoshita,T. and Shinbashi,N. (1982) Identification of dwarf genes and their character expression in the isogenic background. *Jpn J. Breed.*, **32**, 219–231.

Kouchi,H. and Hata,S. (1993) Isolation and characterization of novel nodulin cDNAs representing genes expressed at early stages of soybean nodule development. *Mol. Gen. Genet.*, **238**, 106–119.

Lincoln,C., Long,J., Yamaguchi,J., Serikawa,K. and Hake,S. (1994) A *knotted1*-like homeobox gene in *Arabidopsis* is expressed in the vegetative meristem and dramatically alters leaf morphology when overexpressed in transgenic plants. *Plant Cell*, **6**, 1859–1876.

Long,J.A., Moan,E.I., Medford,J.I. and Barton,M.K. (1996) A member of the KNOTTED class of homeodomain proteins encoded by the *STM* gene of *Arabidopsis*. *Nature*, **379**, 66–69.

Lu,P., Porat,R., Nadeau,J.A. and O'Neill,S.D. (1996) Identification of a meristem L1 layer-specific gene in *Arabidopsis* that is expressed during embryonic pattern formation and defines a new class of homeobox genes. *Plant Cell*, **8**, 2155–2168.

Manak,J.R. and Scott,M.P. (1994) A class act: conservation of homeodomain protein functions. *Dev. Suppl.*, 61–77.

Matsuoka,M., Ichikawa,H., Saito,A., Tada,Y., Fujimura,T. and Kano-Murakami,Y. (1993) Expression of a rice homeobox gene causes altered morphology of transgenic plants. *Plant Cell*, **5**, 1039–1048.

Müller,K.J., Romano,N., Gerstner,O., Garcia-Maroto,F., Pozzi,C., Salamini,F. and Rohde,W. (1995) The barley *Hooded* mutation caused by a duplication in a homeobox gene intron. *Nature*, **374**, 727–730.

Nagao,S. and Takahashi,M. (1963) Trial construction of twelve linkage groups in Japanese rice. Genetical studies on rice plant, XXVII. *J. Fac. Agr. Hokkaido Univ. Sapporo*, **53**, 72–130.

Ohta,S., Mita,S., Hattori,T. and Nakamura,K. (1990) Construction and expression in tobacco of a β-glucuronidase (GUS) reporter gene containing an intron within the coding sequence. *Plant Cell Physiol.*, **31**, 805–813.

Sato,Y., Hong,S.K., Tagiri,A., Kitano,H., Yamamoto,N., Nagato,Y. and Matsuoka,M. (1996) A rice homeobox gene, *OSH1*, is expressed before organ differentiation in a specific region during early embryogenesis. *Proc. Natl Acad. Sci. USA*, **93**, 8117–8122.

Sato,Y., Sentoku,N., Nagato,Y. and Matsuoka,M. (1998) Two separable functions of a rice homeobox gene, *OSH15*, in plant development. *Plant Mol. Biol.*, **38**, 983–998.

Scheres,B., Laurenzio,L.D., Willemsen,V., Hauser,M.T., Janmaat,K., Weisbeek,P. and Benfey,P.N. (1995) Mutations affecting the radial organisation of the *Arabidopsis* root display specific defects throughout the embryonic axis. *Development*, **121**, 53–62.

Schneeberger,R.G., Becraft,P.W., Hake,S. and Freeling,M. (1995) Ectopic expression of the *knox* homeobox gene *rough sheath1* alters cell fate in the maize leaf. *Genes Dev.*, **9**, 2292–2304.

Sinha,N.R., Williams,R.E. and Hake,S. (1993) Overexpression of the maize homeobox gene, *KNOTTED-1*, causes a switch from determinate to indeterminate cell fates. *Genes Dev.*, **7**, 787–795.

Smith,L.G. and Hake,S. (1994) Molecular genetic approaches to leaf development: *Knotted* and beyond. *Can. J. Bot.*, **72**, 617–625.

Smith,L.G., Greene,B., Veit,B. and Hake,S. (1992) A dominant mutation in the maize homeobox gene, *Knotted-1*, causes its ectopic expression in leaf cells with altered fates. *Development*, **116**, 21–30.

Smith,L.G., Jackson,D. and Hake,S. (1995) Expression of knotted1 marks shoot meristem formation during maize embryogenesis. *Dev. Genet.*, **16**, 344–348.

Steeves,T.A. and Sussex,I.M. (1989) *Patterns in Plant Development*. Cambridge University Press, Cambridge, UK.

Takeda,K. (1977) Internode elongation and dwarfism in some gramineous plants. *Gamma Field Sym.*, **16**, 1–18.

Tamaoki,M., Kusaba,S., Kano-Murakami,Y. and Matsuoka,M. (1997) Ectopic expression of a tobacco homeobox gene, *NTH15*, dramatically alters leaf morphology and hormone levels in transgenic tobacco. *Plant Cell Physiol.*, **38**, 917–927.

Vollbrecht,E., Veit,B., Sinha,N. and Hake,S. (1991) The developmental gene Knotted-1 is a member of a maize homeobox gene family. *Nature*, **350**, 241–243.

Received October 15, 1998; revised and accepted December 7, 1998